energies

MDPI

Review

A Review of the Mathematical Models for the Flow and Heat Transfer of Microencapsulated Phase Change Slurry (MEPCS)

Huyu Li [1], Guojun Yu [1,*], Huijin Xu [2,*], Xue Han [3] and Huihao Liu [1]

[1] Merchant Marine College, Shanghai Maritime University, Shanghai 201306, China
[2] China-UK Low Carbon College, Shanghai Jiao Tong University, Shanghai 200240, China
[3] No. 8 Oil Production Plant, Changqing Oilfield Company, Xi'an 710021, China
* Correspondence: gjyu@shmtu.edu.cn (G.Y.); xuhuijin@sjtu.edu.cn or hjxu1015@gmail.com (H.X.)

Abstract: Microencapsulated phase change slurry (MEPCS), prepared by mixing microencapsulated phase change materials (MEPCMs) with water or other carrier fluids, is widely used in different applications such as for thermal regulation or heat storage systems. The transient thermal-hydraulic behavior accompanying the phase change process of the MEEPCS has a significant impact on the system performance. However, the heat and mass transfer during the phase change of the MEPCS is a complex multiscale process, due to the complex phase change of small particles and the complex coupling between the particles and carrier fluids. The numerical methods have been proved to be efficient and powerful means to investigate such complex phase change problems. However, the mathematical model is the critical factor determining the accuracy of the numerical methods, and is still under development. This review summarized the mathematical models proposed for the thermal-hydraulic processes of the MEPCS, compared the adaptabilities of different models, and provided suggestions for the selection of models.

Keywords: microencapsulated phase change slurry; flow and heat transfer; numerical simulation; mathematical model; thermal regulation; thermal storage

Citation: Li, H.; Yu, G.; Xu, H.; Han, X.; Liu, H. A Review of the Mathematical Models for the Flow and Heat Transfer of Microencapsulated Phase Change Slurry (MEPCS). *Energies* **2023**, *16*, 2914. https://doi.org/10.3390/en16062914

Academic Editor: Lyes Bennamoun

Received: 24 February 2023
Revised: 12 March 2023
Accepted: 20 March 2023
Published: 22 March 2023

1. Introduction

Phase change materials (PCMs) are widely utilized in different thermal engineering applications such as thermal regulation and thermal storage, and have become hot topics in energy research [1]. However, some drawbacks of PCMs such as corrosion, volatile, supercooling, and phase segregations restrict their wide application. To overcome these drawbacks, the microcapsule phase change material (MEPCM) is proposed in such a way that the PCMs at the cores are encapsulated in polymer or inorganic shells [2]. These microcapsule particles have different morphologies, such as spherical, irregular shape, single-shell and multi-core, multi-shell and single-core, and matrix rectangle, as shown in Figure 1. However, the most widely used one is the simple spherical morphology [3,4]. MEPCM particles overcome the drawbacks of the PCMs, and also increase the specific surface area of the internal core material, but they are not efficient in heat transfer due to the low conductivity and transport ability. Then, the microencapsulated phase change slurry [5] (MEPCS) was developed by mixing the MEPCM particles with some carrier fluids [6], and the most commonly used carrier fluid is water [7].

The MEPCS is a suspension liquid system that is able to store and transport heat energy, as shown in Figure 2. MEPCS not only has a higher specific heat capacity [8,9], but also has higher thermal conductivity [10] and better flow and heat transfer performance [11] than traditional fluids. Moreover, the melting temperature of the phase change microcapsules can be selected to accommodate specific applications [12]. In addition, it also has good flow performance, which can easily meet the purpose of regulating its flow rate [13,14]. Therefore, MEPCS can be used as a heat transfer fluid and energy storage medium at the

same time, and is widely used in solar collector systems, photovoltaic/thermal systems, air conditioning refrigeration, and heat exchangers and in other fields [15,16].

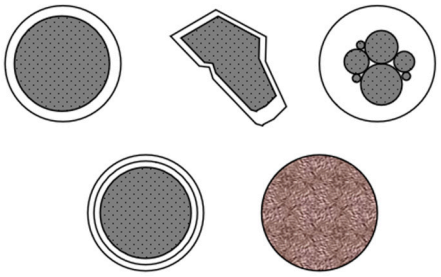

Figure 1. Different morphologies of MEPCM particles [3].

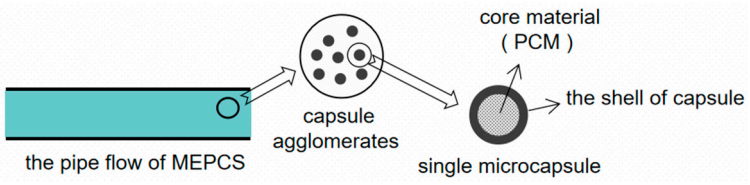

Figure 2. Schematic diagram of the MEPCS [17].

Most of the papers published in the past are related to the application [2,6,11,16,18–20], thermodynamic parameters [6,16,18,21], flow and heat transfer characteristics [6,11,16,18, 19,21–35] of MEPCS. However, it is worth noting that it is basically difficult to observe the complex phase change process inside the capsules by experiment since the size of the microcapsule particles is very small. Therefore, numerical methods are widely used to study the physical processes of the MEPCS, so as to better grasp the phase change mechanism inside the MEPCS and the thermal-hydraulic characteristics of the MEPCS. All numerical studies for MEPCS are based on some assumptions, which make the numerical simulation process easier, but lead to some errors. Therefore, the most challenging problem in the current numerical simulation research of MEPCS is to find a reliable mathematical modeling method, so that more accurate calculations will be realized.

This review paper focused on the mathematical models for the MEPCS that can provide reference for researchers when they are establishing their models. However, to the authors' knowledge, very few review papers about the mathematical models for the MEPCS can be found available in the open literature. In this paper, the research about the mathematical models regarding the thermal and hydraulic processes of the MEPCS will be reviewed and analyzed to provide references for the modeling of the MEPCS, from the following aspects: (1) thermophysical properties of MEPCS; (2) mathematical models for the flow and heat transfer of MEPCS; (3) adaptability analysis and improvement direction of the mathematical model.

2. Methodology

The mathematical models for the MEPCS will be reviewed and analyzed in this paper. Using the search topics of "microencapsulated phase change slurry", "MPCS", "flow and heat transfer", "numerical simulation", and "mathematical model", the literature was retrieved from the "Web of Science" database, focusing on literature published between 2002 and 2022. After the literature collection was completed, 91 high-quality articles were screened out and used for the literature analysis, refining, comparison, and discussion based on abstracts, keywords, and conclusions.

According to the literature analysis, the thermophysical parameters of MEPCS are the basis for the numerical simulation. Therefore, the thermophysical parameters of the MEPCS are described in Section 3 before discussing the mathematical models. Although various studies have been conducted on the MEPCS from the perspective of mathematical models,

they can be basically divided into four categories. More specifically, Section 4.1 reviews the flow and heat transfer studies of the MEPCS based on the single-phase additional heat source. Section 4.2. moves to the second category of the research, the equivalent specific heat capacity modeling for the MEPCS, in terms of the single-phase flow and two-phase flow. Section 4.3 discusses the third category of the research, enthalpy modeling, also in terms of the single-phase flow and two-phase flow. Section 4.4 further discusses the multiscale modeling method. These four categories of studies provide the current advances and major challenges in the mathematical modeling of flow and heat transfer in the MEPCS. On this basis, Section 5 further carries out the adaptability analysis of different mathematical models and puts forward the improvement direction for their future development.

3. Thermophysical Properties of MEPCS

MEPCS can be used as both a heat transfer fluid and energy storage medium. The thermal properties of MEPCS are different from the PCM and carrier fluids. Thermophysical properties of the MEPCS are fundamental for the numerical modeling which then provides guidance for the design of a slurry system. In this section, some important thermophysical parameters of the MEPCS were briefly discussed, including the mass percentage, density, specific heat capacity, thermal conductivity, and viscosity.

3.1. Mass and Volume Percentage

The mass and volume percentages are critical parameters for determining the general properties of the slurry. It is better to introduce the definitions of the mass fraction and volume fraction before introducing the mass percentage and volume percentage. The mass fraction of the MEPCS is defined as the ratio of the mass of the MEPCM particles to the mass of the slurry, expressed by w. Similarly, the volume fraction is defined as the ratio of the volume of the particles to that of the slurry, indicated by ϕ. The correlation between the volume fraction and mass fraction of MEPCS is given by Equation (1). If the mass fraction and volume fraction are denoted by the symbol %, they are referred to as mass percentage and volume percentage. Some researchers habitually say mass concentration instead of mass percentage. This is not accurate, because the mass concentration is the ratio of the mass of the solute to the total volume of the solution.

$$\phi = w\frac{\rho_s}{\rho_p} \tag{1}$$

where ρ_s and ρ_p represent the density of the slurry and MEPCM particles, respectively. Due to the phase transition effect in the slurry, the mass percentage also has a great influence on other thermophysical properties of the MEPCS, such as the viscosity, specific heat capacity, and thermal conductivity.

Studies have shown that the specific heat and thermal conductivity of the MEPCS decrease with the increase in the mass percentage in the region before and after the phase transition [36]. In the region where phase transition occurs, with the absorption and release of more latent heat during the phase change, the specific heat of the slurry increases with the increase in mass percentage, and the influence of the mass percentage on the thermal conductivity still needs further study [37]. In addition, the viscosity of the slurry also increases with the mass percentage, because more MEPCM particles makes the MEPCS change from a Newtonian fluid to a non-Newtonian fluid [38].

3.2. Density

Since the MEPCS is a mixed liquid composed of the MEPCM particles and carrier fluid, and the MEPCM particles are composed of a core and shell, its density is related to the density of the two components. That is, the density of the slurry (ρ_s) is related to the density of the MEPCM particles (ρ_p), the density of the core material (ρ_c), the density of the shell (ρ_w), the density of the carrier fluid (ρ_f), and the mass fraction (w). Therefore, the densities

of the slurry and the particles can be defined by Equations (2) and (3) in accordance with the mass conservation [6]:

$$\rho_s = \frac{\rho_p \rho_f}{w\rho_f + (1-w)\rho_p} \tag{2}$$

$$\rho_p = \frac{(1+y)\rho_c \rho_w}{\rho_c + y\rho_w} \tag{3}$$

In Equation (3), y represents the weight ratio of the core–shell. In general, the density of the microcapsule particles is similar to that of the carrier fluid, which ensures the static stability of the MEPCS. Although the density of the core material usually changes by 10~15% during the phase change process, the change in the density of the slurry is less than 1~2% at a low mass percentage, which can be treated as a constant in calculations [39].

3.3. Specific Heat Capacity

Due to the phase change effect, the MEPCS can be used as either a heat transfer fluid or an energy storage medium, and is widely used in various fields. In order to analyze the effect of the phase transition, the specific heat capacity of the slurry (C_s) should be discussed.

The definition of the specific heat of the microcapsule particles is similar to that of the particle density, which is also related to the specific heat of the core material and shell. That is, the specific heat of the slurry (C_s) is related to the specific heat of the microcapsule particles (C_p), the specific heat of the core material (C_c), the specific heat of the shell (C_w), the specific heat of the carrier fluid (C_f), and the mass fraction (w). Therefore, the specific heats of the slurry and the particles are given by Equations (4) and (5) [40]:

$$C_s = wC_p + (1-w)C_f \tag{4}$$

$$C_p = \frac{(yC_c + C_w)\rho_c \rho_w}{\rho_p(\rho_c + y\rho_w)} \tag{5}$$

In some numerical modeling, an effective specific heat capacity is defined to simplify the treatment of the phase change, in which the effect of the phase change is incorporated in this effective specific heat capacity. Then, the specific heat capacity of the slurry presents three stages during the whole phase change process, as shown in Figure 3. The specific heat of the slurry is considered to be constant in the stages before and after the phase transition, which is equivalent to the weight-average specific heat of the particle and the carrier fluid. In these two stages, the specific heat of the slurry decreases with the increase in the mass percentage [36] of the particle, as shown in Equation (4). However, during the phase change process from temperature T_1 to T_2, the specific heat of the slurry not only includes the effect of the latent heat H of the capsule, but also the effect of the specific heat of the particle and the carrier liquid, so the specific heat of the slurry is much larger than that of the other two stages. Based on this simplification, the effective specific heat of the slurry can be given by Equation (6) [41].

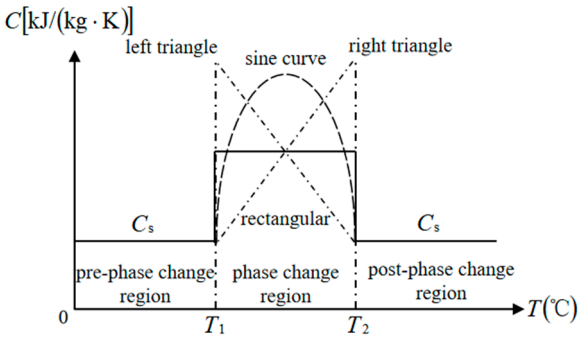

Figure 3. Variation curve of specific heat capacity of slurry versus phase transition temperature [6].

Therefore, the final expression of the specific heat capacity of the slurry in the phase transition temperature range is as follows [41]:

$$C_s(T) = \begin{cases} C_s & \text{If } T < T_1 \\ C_s + \frac{H}{T_2 - T_1} & \text{If } T_1 \le T \le T_2 \\ C_s & \text{If } T > T_2 \end{cases} \quad (6)$$

3.4. Thermal Conductivity

The thermal conductivity of the MEPCM particles can be calculated based on the composite sphere method [42]:

$$\frac{1}{k_p d_p} = \frac{1}{k_c d_c} + \frac{d_p - d_c}{k_w d_p d_c} \quad (7)$$

$$\left(\frac{d_p}{d_c}\right)^3 = 1 + \frac{\rho_w}{\rho_w + y\rho_c} \quad (8)$$

The thermal conductivity of MEPCS can be calculated by the classical Maxwell relations [43]:

$$k_s = k_f \frac{2 + k_p/k_f + 2\phi(k_p/k_f - 1)}{2 + k_p/k_f - \phi(k_p/k_f - 1)} \quad (9)$$

where, the subscripts c, w, p, f, and s represent the core material, shell, capsule particles, carrier fluid, and slurry respectively.

It is noteworthy that Equation (9) is only applicable to the static conditions. However, in the case of flow, the thermal conductivity of the MEPCS will increase due to the interaction between the particles and carrier fluid. Therefore, the thermal conductivity (k_s) calculated by the classical Maxwell relationship is lower than the effective thermal conductivity (k_e) under flow conditions, and the correlation between them is as follows [24]:

$$k_e = k_s \cdot (1 + B\phi Pe_p)^m \quad (10)$$

$$Pe_p = \frac{\vec{e}\, d_p{}^2}{\alpha_f} \quad (11)$$

$$\begin{cases} B = 3.0\ m = 1.5 & Pe_p < 0.67 \\ B = 1.8\ m = 0.18 & 0.67 \le Pe_p \le 250 \\ B = 3.0\ m = 1/11 & Pe_p > 250 \end{cases} \quad (12)$$

where the Peclet number (Pe_p) indicates the relative magnitude between the convection and diffusion of the microcapsule particles, which is related to the MEPCM particle diameter (d_p), thermal diffusion coefficient (∂_f), and shear rate ($\vec{e}$). In Equation (10), the range of Pe_p determines the values of B and m.

Generally, the enhanced heat transfer of the MEPCS is caused by the absorption or release of the latent heat during the phase change in the microcapsules and by the increase in the effective thermal conductivity of the slurry. The higher the effective thermal conductivity of slurry is, the greater the heat transfer rate is. Yuan et al. [44] prepared the MEPCS by uniformly dispersing 10 wt% microcapsule particles into water, and found that the thermal conductivity of the MEPCS was increased by 6.5% compared to the water. Liu et al. [45] found that the thermal conductivity of the MEPCS increases with the Reynolds number, and the thermal conductivity of the MEPCS can reach 2~3 times that of the traditional single-phase fluid under the same Reynolds number.

3.5. Viscosity

The viscosity of the MEPCS plays an important role in determining the pressure drop and the pumping power of the conveyor during the flow process. The greater the viscosity,

the greater the pressure drop and the higher the pumping power will be, which is not conducive to the practical application of the MEPCS. Some studies have shown that the MEPCS behaves as a Newtonian fluid when its mass percentage is below 25% [7,46,47], or when the viscosity varies linearly with the shear rate [36]. Most of the viscosity and shear rate curves of the MEPCS were measured experimentally using the rheometers [12,48,49]. The "Optimal Viscosity-Shear rate" tool of the rheometer software can be used to provide the behavior equation between the viscosity and shear rate. The equation that best predicts the shape of the flow curve of the MEPCS has been found to be the Caro model [50], which is defined according to Equation (13):

$$\frac{\mu_s - \mu_\infty}{\mu_0 - \mu_\infty} = \frac{1}{\left(1 + (k \cdot \dot{\gamma})^2\right)^{m/2}} \tag{13}$$

where, $\dot{\gamma}$ is the shear rate, μ_0 and μ_∞ represent the asymptotic value of the viscosity at very low and very high shear rates respectively, k is a constant parameter in the dimension of time, and m is a dimensionless constant. The values of these constants can be obtained from Ref. [50].

In addition, at low mass percentages, the MEPCS can be regarded as a homogeneous fluid, and thus its viscosity can also be calculated according Equation (14), which includes the influence of the interaction between the MEPCM particles, carrier fluid, and tube wall [51].

$$\frac{\mu_s}{\mu_f} = \left(1 - \phi - A\phi^2\right)^{-2.5} \tag{14}$$

where, $\frac{\mu_s}{\mu_f}$ is the relative viscosity and is defined by the ratio of the apparent viscosity of the MEPCS to that of the water at a given temperature. A is a parameter that depends on the size, shape, and stiffness of the MEPCM particles. Mulligan et al. [52] showed that the value of A for the MEPCS is 3.4 when the capsule particle diameter is 10~30 μm. In the study of Wang et al. [53], the value of A is found to be 4.45 for an average capsule diameter of 10.112 μm at different mass percentages. However, Charunyakorn et al. [24] found that the value of A is 1.16 when the mass percentage of the slurry is less than 20%. They measured the relative viscosity of the MEPCS at different mass percentages and found that the curve fit the function well, proving the validity of Equation (14).

4. Mathematical Models for Flow and Heat Transfer of the MEPCS

In terms of flow, the existing common models for the MEPCS are mainly divided into the single-phase flow model [54] and two-phase flow model [55]. With regard to the heat transfer, the existing phase-change heat transfer models for the MEPCS are mainly divided into three categories, namely, the additional heat source model [24], equivalent specific heat capacity model [27], and the enthalpy model [26]. Different mathematical models for the MEPCS can be established by combining different flow models with different heat transfer models. To the authors' knowledge, the mathematical models for the thermal and hydraulic behavior of the MEPCS can be divided into five categories: the single-phase additional heat source model, single-phase equivalent specific heat capacity model, two-phase equivalent specific heat capacity model, single-phase enthalpy model, and two-phase enthalpy model. In addition, some researchers have proposed multiscale models for the flow and heat transfer process of MEPCS [34,56,57]. In this section, these mathematical models for the MEPCS will be reviewed and compared, to provide guidance for the numerical modeling.

4.1. Single-Phase Additional Heat Source Model

The single-phase additional heat source model is one that considers the flow of the MEPCS as a single-phase flow and introduces the phase change by an additional heat source. The so-called single-phase flow, as the name implies, means that the differences in the phase state (solid phase, liquid phase, and gas phase) during the flow of the fluid

are not considered [58]. Because the size of the suspended MEPCM particles in MEPCS is very small [59], and these microcapsules are easily fluidized, some researchers describe the MEPCS as a homogeneous single-phase fluid, with the average thermal physical properties used. In this single-phase model, it can be assumed that both the solid phase (MEPCM particles) and liquid phase (carrier fluid) are in thermal equilibrium, and the slip motion between the carrier fluid and MEPCM particles can be ignored [60]. Therefore, in this single-phase model, the governing equations of the MEPCS are similar to those of traditional uniform fluids. The additional heat source refers to the heat generated or absorbed during the phase change of the MEPCM particles as an additional internal heat source related to the fluid temperature in the carrier fluid. This additional model is usually obtained by an ideal modeling phase change rate. The governing equations in the framework of this modeling usually include the continuity equation, momentum equations, and energy equation. In some situations, the continuity and momentum equations can be simplified due to the feature of the flow. A heat source is added to the energy equation to incorporate the effect of the phase change, which is usually derived by assumption. Equations (15)–(17) show the governing equations proposed by Charunyakorn et al. [24] for the flow and heat transfer of MEPCS in a circular tube, where Equation (17) is the ideal additional heat source added to the energy equation.

$$u_x = 2u_m\left[1-(r/R)^2\right] \tag{15}$$

$$\rho c_p u_x \frac{\partial T}{\partial x} = \frac{\partial}{\partial r}\left(k\frac{\partial T}{\partial r}\right) + \left(\frac{k}{r}\frac{\partial T}{\partial r}\right) + \frac{\partial}{\partial x}\left(k\frac{\partial T}{\partial x}\right) + \mu\left(\frac{\partial u}{\partial r}\right)^2 + S \tag{16}$$

$$S = 3\varphi_S k_\mathrm{p}\frac{(T_m - T)}{r_\mathrm{p}^2}\frac{r_\mathrm{m}}{r_\mathrm{p}-(1-\beta)r_\mathrm{m}} \tag{17}$$

The single-phase additional heat source model has the advantages of having a simple conception, easy implementation, and good computational efficiency, but its limitations are also very prominent: when the capsule particle size is large or the density difference between the capsule and the carrier fluid is large, MEPCS is not a homogeneous fluid, and the homogeneous assumption will cause significant error; in addition, the accuracy of the model is decided by the heat source, which is not easily obtained. Although the single-phase additional heat source modeling is simplified, it is useful and convenient. With this model, the influences of some parameters of the system, such as the Stefan number, mass percentage, particle size, Reynolds number, inlet subcooling, and other parameters on the flow and heat transfer can be investigated.

Charunyakorn et al. [24] numerically studied the influence of the Stefan number, mass percentage, and particle size on the flow and heat transfer characteristics of MEPCS in a circular tube. The calculation results were validated by the experimental results [61], indicating that the deviation between the calculated average Nusselt number of the slurry and the experimental data was between 6% and 12%. In addition, Qiu et al. [25] also used the single-phase additional heat source model to study the flow and heat transfer characteristics of MEPCS in a circular tube under constant heat flux. The results showed that the average deviation between the calculated dimensionless wall temperature of MEPCS and the experimental data was less than 5%.

4.2. Equivalent Specific Heat Capacity Model

The second thermal-hydraulic model for the MEPCS is the equivalent specific heat capacity model [62], in which the effect of the phase change of the MEPCM particles is described by the change in the specific heat capacity of the MEPCS. The effective specific heat capacity of the slurry is determined from the correlation between the temperature and enthalpy, as shown in Equation (6). The correlation between the enthalpy and temperature can be determined by a differential scanning calorimeter (DSC) measurement.

This modeling method is easy to implement and avoids the application of complex source terms in the mathematical model to deal with the phase change process, and can achieve acceptable accuracy for some calculations, but this modeling method has its inherent shortcomings: the equivalent specific heat capacity model does not behave well when the phase change temperature range is small, and is not suitable for the step phase change problems. In addition, the equivalent specific heat capacity model is based on the assumption of a "homogenization temperature" inside the capsule, which oversimplifies the specific phase change process inside the capsule and sometimes results in a significant error. Depending on the description of the flow, the equivalent specific heat capacity model includes the single-phase equivalent specific heat capacity model and two-phase equivalent specific heat capacity model.

4.2.1. Single-Phase Equivalent Specific Heat Capacity Model

The single-phase equivalent specific heat capacity model treats the MEPCS as a homogeneous single-phase fluid, and the phase change process in the capsule is modeled by the equivalent specific heat capacity method. Sometimes the MEPCM particles are well dispersed in the carrier fluid, and treating the MEPCS as a homogeneous fluid does not cause too much error. Therefore, this modeling method is widely used. The governing equations in the framework of this modeling approach usually include the continuity equation, momentum equations, and energy equation. Equations (18)–(20) show the governing equations proposed by Seyf et al. [63], where $c_{p,\mathrm{eff}}$ is the effective specific heat capacity incorporating the phase change effect of the MEPCS and can be obtained from some correlations such as Equation (6).

$$\nabla \cdot \boldsymbol{u} = 0 \tag{18}$$

$$\rho_{\mathrm{eff}} \nabla \cdot (\boldsymbol{u}u) = -\nabla p + \mu_{\mathrm{eff}} \nabla \cdot \left(\nabla u + \nabla u^{\mathrm{T}} \right) \tag{19}$$

$$\rho_{\mathrm{eff}} c_{p,\mathrm{eff}} \nabla \cdot (\boldsymbol{u}T) = \nabla \cdot (k_{\mathrm{eff}} \nabla T) + \Phi^2 \tag{20}$$

Hu et al. [27] conducted a numerical simulation study on the laminar forced convection heat transfer of the MEPCS in a circular tube with constant heat flow, based on the single-phase equivalent specific heat capacity model. The numerical results were compared with the experimental results [39], showing that the maximum relative error was 6%. It is found that the Stefan number and mass percentage are the most important parameters for improving the flow and heat transfer of the MEPCS, which is consistent with the research results of Charunyakorn and Qiu using the single-phase additional heat source model [24,25]. The difference is that the heat transfer enhancement effect increases with the decrease in the dimensionless initial subcooling and dimensionless phase change temperature range, and increases with the increase in the particle size. Languri et al. [28] studied the turbulent flow and heat transfer of the MEPCS in the spiral heat exchanger, using the equivalent specific heat capacity modeling. The maximum deviation between the calculated average Nusselt number and the experimental data [64] was 5%. In addition, Ran et al. [65] established a single-phase equivalent specific heat capacity model to study the turbulent flow and heat transfer of the MEPCS in a two-wheel spiral tube under constant wall heat flux conditions. The numerical results were compared with the experimental data [46], indicating a good agreement with the experimental data. Shaukat et al. [66] numerically studied the laminar flow and heat transfer of the MEPCS in the microchannel radiator using the single-phase equivalent specific heat capacity model. The maximum deviation between the calculated local Nusselt number and the experimental data [10] was found to be 14.6%.

The advantage of this modeling lies in the fact that it is a pure macroscopic model, which describes the flow and heat transfer for the whole solution, and does not need to track the solid–liquid interface. It is widely used due to its easy implementation, small computation cost, and fast calculation speed. However, the limitation is that the modeling

ignores the interaction between the microcapsule and the carrier fluid, oversimplifying the phase change process of the microcapsule and the temperature distribution in the microcapsule, which inevitably causes certain deviations in most cases.

4.2.2. Two-Phase Equivalent Specific Heat Capacity Model

Although the single-phase flow model is simple in the modeling and efficient in the numerical calculation, it is not accurate enough for some calculations, since it does not accurately consider the interaction between the carrier fluid and microcapsule particles, as well as the particle sedimentation and dispersion under the influence of gravity. The MEPCS is essentially a two-phase fluid, therefore, the classical two-phase flow models have been used to describe the flow and heat transfer of the slurry. In the two-phase models, the microcapsule particles and the carrier fluid are considered to be two different phases with different velocities and temperatures, and the assumption of zero slip velocity between the two phases is no longer valid. Among these two-phase models, the Euler model is widely used. The two-phase flow models describe the role of solid–liquid two-phase in the flow and heat transfer process [67,68]. In the framework of this modeling, the governing equations, continuity, momentum, and energy are established for the solid and liquid phase separately. Similarly, the phase change effect is incorporated by an effective specific heat capacity. Equations (21)–(23) are those constructed by Ma et al. [69] for the thermo-fluidic performance of the MEPCS and energy transport characteristics.

$$\frac{\partial(\alpha_i\rho_i)}{\partial t} + \nabla\cdot(\alpha_i\rho_i v_i) = 0 \tag{21}$$

$$\frac{\partial(\alpha_i\rho_i v_i)}{\partial t} + \nabla\cdot(\alpha_i\rho_i v_i v_i) = -\alpha_i\nabla P - \nabla P_s + \nabla\cdot\bar{\bar{\tau}}_i + \alpha_i\rho_i g + F_{D,i} + F_{L,i} + F_{td,i} \tag{22}$$

$$\frac{\partial\left(\alpha_i\rho_i c_{p,p,e}T_i\right)}{\partial t} + \nabla\cdot\left(\alpha_i\rho_i v_i c_{p,p,e}T_i\right) = \nabla\cdot(\lambda_{e,i}\nabla T_i) + \bar{\bar{\tau}}_i : \nabla v_i - h_{sl}\left(T_i - T_q\right) \tag{23}$$

where the subscripts i= l or i= s represent the liquid phase or solid phase, and the last term of Equation (23) represents the heat transfer between the two phases. The latent heat of the MEPCS is regarded as the effective specific heat capacity ($c_{p,p,e}$), which is given by Equation (24).

$$\int_{T_{p,s}}^{T_{p,l}} c_{p,p,e}dT = \Delta H_p + \frac{c_{p,p,s} + c_{p,p,l}}{2}\left(T_{p,l} - T_{p,s}\right) \tag{24}$$

Compared with the single-phase equivalent specific heat capacity models, the two-phase equivalent specific heat capacity models can describe the heterogeneous flow of the slurry; therefore, they are more accurate in most cases. However, they require a significant computational cost compared to the single-phase model. In addition, the phase change process inside the capsule is still oversimplified in this two-phase equivalent specific heat capacity model, since the "homogenization temperature" hypothesis inside the microcapsule is used. However, the two-phase equivalent specific heat capacity model is found to be accurate enough for some engineering calculations.

Bai et al. [29] numerically studied the laminar heat transfer process of MEPCS in a circular tube with constant wall heat flux using the two-phase equivalent specific heat capacity model. Their numerical results showed agreement with the experimental data in [40], and the two-phase model was found to be more accurate than the single-phase model. Xin et al. [70] conducted a numerical study on the turbulent heat transfer process of MEPCS in a circular tube with a constant wall heat flux, based on the two-phase equivalent specific heat capacity model. The numerical results were found to agree well with the experimental data reported in Ref. [39], with the maximum relative error being less than 14%. Wu et al. [71] studied the flow and heat transfer behavior of the slurry in a horizontal circular tube under a constant wall heat flux. The results were found to agree well with the experimental data from Ref. [72]. In the research from Wu et al., the authors also compared the two-phase model and single-phase model for the computation performance.

The results showed that the assumption of the uniform distribution of the particles for the single-phase flow model was not reasonable, since the particle distribution was found to affect the temperature distribution. The single-phase model ignores the interaction between the particles and the carrier fluid, which reduced the accuracy of the calculation. It was also found that the deviation in the calculated results between the single-phase model and two-phase model increased with the increase in mass concentration. In addition, Liu et al. [35] established the two-phase equivalent specific heat capacity model for the laminar forced convection of the MEPCS. The calculated results for the circular tube flow was found to be in good agreement with the experimental data [24], and the maximum relative error of 10% was obtained for the rectangular tube flow case compared with the experimental data in Ref. [73].

Dai et al. [30] established a two-phase equivalent specific heat capacity model for the heat and mass transfer in a two-layer microchannel with MEPCS as the working fluid. The computation results were compared with the experimental data from [10,74,75], indicating that the computation results agreed well with the experimental data, with the deviation being less than 1 %. Moreover, Dai et al. [76,77] also established the two-phase equivalent specific heat capacity models for the MEPCS in the porous media microchannels, also with good accuracy.

4.3. Enthalpy Model

The enthalpy model [62] is one in which a unified energy equation is constructed for the whole PCM (including the liquid phase, solid phase, and two-phase interface of the PCM) by introducing the concept enthalpy. By introducing the enthalpy model, the phase change problem becomes much easier because the energy equations for the different phases of the PCM are unified to the same form, and explicit boundary conditions on the phase change interface are not required, which means that the numerical computation can be performed on a fixed grid.

The total enthalpy of the slurry H is defined by the sum of the sensible heat and latent heat of the slurry, as shown in Equation (25).

$$H = h_{\mathrm{e}} + \Delta h \tag{25}$$

The sensible heat h_{e} of slurry is given by Equation (26), where h_{ref} is the reference enthalpy at T_{ref}.

$$h_{\mathrm{e}} = h_{\mathrm{ref}} + \int_{\mathrm{T_{ref}}}^{\mathrm{T}} C_{\mathrm{s}} \mathrm{d}T \tag{26}$$

The latent heat of slurry Δh is represented by Equation (27), where L is the latent heat of the phase change material, φ is the mass percentage of particles in the MEPCS, and β is the volume fraction of the liquid phase in the capsule. The PCM starts melting at T_{solidus} and becomes completely melted at T_{liquidus}, and the liquid fraction varies from zero at T_{solidus} to one at T_{liquidus}, which can be expressed by Equation (28).

$$\Delta h = \beta \varphi L \tag{27}$$

$$\beta = \begin{cases} 0 & \text{If } T < T_{\mathrm{solidus}} \\ \frac{T - T_{\mathrm{solidus}}}{T_{\mathrm{liquidus}} - T_{\mathrm{solidus}}} & \text{If } T_{\mathrm{solidus}} \le T \le T_{\mathrm{liquidus}} \\ 1 & \text{If } T > T_{\mathrm{liquidus}} \end{cases} \tag{28}$$

The enthalpy model is the most widely used one to investigate the phase change process of the MEPCS, since it is very simple to be implemented. Moreover, the enthalpy modeling can be performed with a lower computational cost since the specific heat capacity–temperature test is not necessary. However, as is similar to the equivalent specific heat capacity model, the enthalpy model adopts the assumption of "homogenization temperature" for the phase change process inside the capsule, which oversimplifies the phase

change process inside the capsule. In addition, it is difficult to deal with the phase change problems using supercooling and temperature oscillations. In the framework of the enthalpy method, the single-phase enthalpy model and two-phase enthalpy model are widely used.

4.3.1. Single-Phase Enthalpy Model

The single-phase enthalpy model regards the MEPCS as a homogeneous single-phase fluid, and the phase change in the capsule is described by the change in enthalpy. Since this modeling is very simple, it has been widely employed in various research. The construction of the single-phase enthalpy model is very similar to that of the single-phase equivalent specific heat capacity model. The main difference lies in the treatment of the latent heat of the phase transition in the energy equation. The continuity and momentum equations are similar with those shown in Equations (18) and (19), while the energy equation is given in terms of the enthalpy, as shown in Equation (29) with the example of the steady-state case [32]:

$$\nabla \cdot [u(\rho_L H)] = \nabla \cdot (k_{\text{eff}} \nabla T_L) \tag{29}$$

where, the value of H can be referred to in Equation (24).

Inaba et al. [78] established a single-phase enthalpy model to study the thermal storage and heat transfer behavior of the MEPCS in a horizontal rectangular shell; the deviation between the numerical results and experimental data was found to be 10%. Zeng et al. [31] also constructed the single-phase enthalpy model to study the convective heat transfer behavior of the MEPCS flowing in a circular tube; the calculated Nusselt number was validated by the experimental data, with a deviation of 9.4%. In addition, Sabbah et al. [32] established a three-dimensional, single-phase enthalpy model to study the laminar flow and heat transfer performance of a microchannel heat sink with MEPCS as the coolant; the numerical results were found to be in good agreement with the experimental data from Ref. [40]. Hasan [79] established the single-phase enthalpy model for the MEPCS in a counterflow microchannel heat exchanger and validated the numerical results by the experimental data from Ref. [80], with the deviation being 2.1%.

The single-phase enthalpy models are of the macroscopic models, so they have the advantages of easy implementation and fast operation. However, they do not get rid of the limitation of the macroscopic model, i.e., it is difficult to consider the phase change process of the capsule in detail. When dealing with the phase change process in the capsule, they still ignore the temperature gradient inside the capsules, that is, they still follow the "homogenization temperature" hypothesis. In addition, the single-phase enthalpy model does not take into account the interaction between the capsule and the carrier fluid, which may cause large deviations in some situations.

4.3.2. Two-Phase Enthalpy Model

The main idea of the two-phase enthalpy model is to regard the carrier fluid and capsule particles in the MEPCS as two interacting continuous fluids. The two-phase enthalpy model is also a macroscopic one, which establishes the mass, momentum, and energy conservation equations for the solid and liquid phases respectively, making the phase interaction and thermal-hydraulic process more intuitive and clear. However, since the conservation equations are established for the solid and liquid phases separately, the calculation amount for solving this model is approximately twice that of the single-phase enthalpy model, resulting in larger computation cost as well as poor numerical stability. Although the two-phase enthalpy models have the same limitations as the single-phase enthalpy models in simplifying the phase change process in the capsule, they are generally much more attractive than the other models mentioned above, and are widely used in various research. In the framework of this modeling, the continuity, momentum, and energy equations are established for different phases, i.e., the carrier fluid (liquid phase) and microcapsule particles (solid phase). Equations (30)–(35) show the governing equations established for the flow and heat transfer of MEPCS in a wide rectangular microchannel,

by Abhijith et al. [81]. In these equations, the subscript s indicates that this equation is provided for the PCM in the microcapsule particles, and l indicates that this equation is provided for the carrier fluid.

$$\frac{\partial(\varepsilon_l \rho_l)}{\partial t} + \nabla \cdot (\varepsilon_l \rho_l v_l) = 0 \tag{30}$$

$$\frac{\partial(\varepsilon_s \rho_s)}{\partial t} + \nabla \cdot (\varepsilon_s \rho_s v_s) = 0 \tag{31}$$

$$\begin{aligned} \tfrac{\partial(\varepsilon_l \rho_l v_l)}{\partial t} + \nabla \cdot (\varepsilon_l \rho_l v_l v_l) = {} & -\varepsilon_l \nabla p + \nabla \cdot \left[\varepsilon_l \mu_l \left(\nabla v_l + \nabla v_l^T\right)\right] \\ & + \varepsilon_l \rho_l g - F_d + F_{\mathrm{vm}} \end{aligned} \tag{32}$$

$$\begin{aligned} \tfrac{\partial(\varepsilon_s \rho_s v_s)}{\partial t} + \nabla \cdot (\varepsilon_s \rho_s v_s v_s) = {} & -\varepsilon_s \nabla p + \nabla \cdot \left[\varepsilon_s \mu_s \left(\nabla v_s + \nabla v_s^T\right)\right] \\ & + \varepsilon_s \rho_s g + F_d - F_{\mathrm{vm}} - F_{\mathrm{par}} \end{aligned} \tag{33}$$

$$\begin{aligned} \tfrac{\partial(\varepsilon_l \rho_l i_l)}{\partial t} + \nabla \cdot (\varepsilon_l \rho_l v_l i_l) = {} & -p\left[\tfrac{\partial \varepsilon_l}{\partial t} + \nabla \cdot (\varepsilon_l v_l)\right] + \nabla \cdot (\varepsilon_l k_{\mathrm{eff},l} \nabla T_l) \\ & - h_v (T_l - T_s) \end{aligned} \tag{34}$$

$$\begin{aligned} \tfrac{\partial(\varepsilon_s \rho_s i_s)}{\partial t} + \nabla \cdot (\varepsilon_s \rho_s v_s i_s) = {} & -p\left[\tfrac{\partial \varepsilon_s}{\partial t} + \nabla \cdot (\varepsilon_s v_s)\right] + \nabla \cdot (\varepsilon_s k_{\mathrm{eff},s} \nabla T_s) \\ & + h_v (T_l - T_s) \end{aligned} \tag{35}$$

Hao et al. [26] established a two-phase enthalpy model for the MEPCS laminar flow in microchannels. This model was found to be able to describe the separation of the solid–liquid flow and the coupling between thermal diffusion, convection, and inter-particle interactions. The numerical results were found to be consistent with the experimental observations and measurement results. Afterwards, Xing et al. [33] used the same model to investigate the laminar flow and heat transfer of the MEPCS in the microchannels; the numerical results were compared with experimental data in Ref. [61], showing a deviation of 3.8%. In addition, Lian et al. [82] also used the two-phase enthalpy model to study the cooling performance of the MEPCS applied to the liquid-cooled plate; the numerical results were found to agree well with experimental data in Ref. [10].

4.4. Multiscale Model

The MEPCS shows multiscale behavior during various applications in either latent heat storage or thermal regulation. The multiscale of the MEPCS is shown in Figure 4 [34]. On the slurry scale, a large number of microcapsule particles are suspended in the carrier fluid, showing the macroscopic heat transfer characteristics of a single-phase fluid or two-phase fluid [83]; on the agglomeration scale, the temperature distribution is uneven in a local small area, and the microcirculation convection is found in a local region [7]; on the particle scale, the complex phase change process of the core material inside the capsule and the interaction between the capsules and the carrier fluid show local-based behavior [84]. At the nanoscale, the movement of the molecules defines the phase change of the core material.

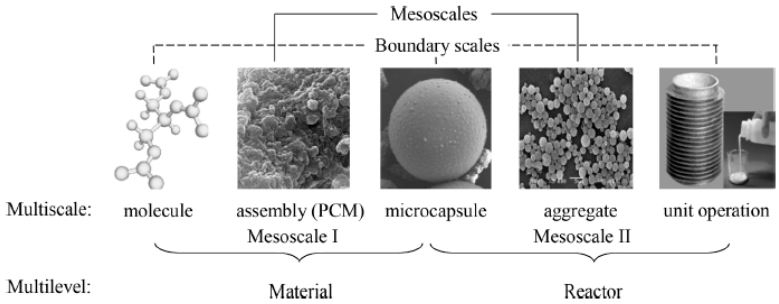

Figure 4. Multiscale in the field of microencapsulated phase change material slurry [34].

In the single-phase and two-phase models discussed above, all thermo-physical properties of the MPCM and the temperature distribution inside the microcapsules area are assumed to be identical. Therefore, the energy exchange between the capsule and carrying fluid is linear during the phase change of the MPCM, which goes against the findings in some research [84–86]. Obviously, it is difficult to acquire a comprehensive understanding of the heat and mass transfer behavior of the MPCM slurry using the models mentioned above; and it is necessary to construct the multiscale models for the heat and mass transfer of MEPCS in different applications.

At present, there is very little literature on the numerical simulation of the MEPCS flow and heat transfer using the multiscale model. Lin et al. [34] developed a multiscale model for the MPCM slurry by combining the heterogeneous multiscale method framework [87] and the correlative multiscale methodology [88]. The idea of the development for this correlation multiscale coupling model is shown by the Figure 5, in which U and u indicate the macroscopic and microscopic variables, and F and f are symbols of the macroscale and microscale models. The missing data in the macroscale model are represented by X, which will be provided by the microscale model. Meanwhile, the constraint x for the microscale model will be provided by the macroscopic model. For the MEPCS, X can be defined as the heat source term caused by the phase change of the microcapsule particles in the macroscopic slurry model. Moreover, x is defined as the phase transition state of the core material inside the capsule and thermal boundary condition outside the capsule, that is, the condition constraint from the macroscopic slurry scale on the microscopic capsule scale. In their microscale model, which was based on a lattice Boltzmann model, is used to calculate the microscopic phase change of the MPCM.

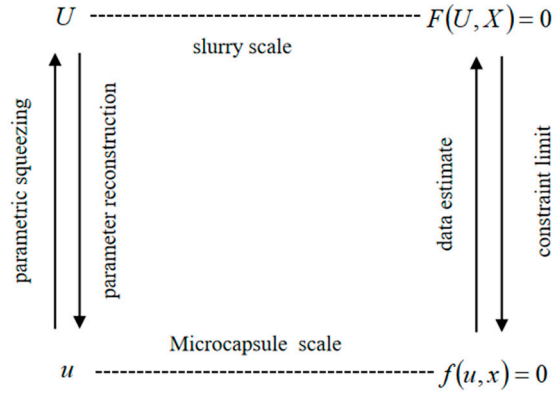

Figure 5. Overall construction framework of correlation multiscale coupling model [34].

In the framework of the multiscale model, the governing equations are constructed for both the macroscale and the microscale, and the information between the two scales is then exchanged by a certain method. The governing equations in the macroscale can be established by the methods mentioned above, and the microscale can be established by the lattice Boltzmann method or the molecular dynamics method. Equations (36)–(42) show the governing equations for the macroscale and microscale for the flow and heat transfer of MEPCS in a circular tube, by Lin et al [34].

The governing equations for the macroscale are:

$$\frac{\partial}{\partial t}(\varphi_L \rho_L) + \nabla \cdot (\varphi_L \rho_L u_L) = 0 \tag{36}$$

$$\frac{\partial}{\partial t}(\varphi_S \rho_S) + \nabla \cdot (\varphi_S \rho_S u_S) = 0 \tag{37}$$

$$\begin{aligned} \tfrac{\partial}{\partial t}(\varphi_L \rho_L u_L) + \nabla \cdot (\varphi_L \rho_L u_L u_L) = \; & -\varphi_L \nabla p + \nabla \cdot \left[\varphi_L \mu_L \left(\nabla u_L + \nabla u_L^T\right)\right] \\ & + \varphi_L \rho_L g + F_{SL} \end{aligned} \tag{38}$$

$$\frac{\partial}{\partial t}(\varphi_S \rho_S u_S) + \nabla \cdot (\varphi_S \rho_S u_S u_S) = \begin{array}{l} -\varphi_S \nabla p - \nabla p_S + \nabla \cdot \left[\varphi_S \mu_S \left(\nabla u_S + \nabla u_S^T\right)\right] \\ +\varphi_S \rho_S g - F_{SL} \end{array} \quad (39)$$

$$\frac{\partial}{\partial t}(\varphi_L \rho_L T_L) + \nabla \cdot (\varphi_L \rho_L u_L T_L) = \nabla \cdot \left[\left(\lambda_L / c_p\right) \nabla T_L\right] + \dot{Q}_{SL} \quad (40)$$

The governing equations for the microscale are:

$$f_i^*(x + \delta_x, t + \delta_t) = f_i(x,t) - \left[f_i(x,t) - f_i^{eq}(x,t)\right] \Big/ \tau_f + \left(1 - 0.5\omega_f\right) \delta_t S_{f,i}(x,t) \quad (41)$$

$$g_i(x + \delta_x, t + \delta_t) = g_i(x,t) - \left[g_i(x,t) - g_i^{eq}(x,t)\right] \Big/ \tau_g \quad (42)$$

where, $\dot{Q}_{SL}$ represents the heat transfer capacity between the two phases involved in the phase transition in the microcapsule, whose value can be calculated by obtaining the shell temperature of the microcapsule or the phase transition rate in the microcapsule from the simulation results at the microcapsule scale.

However, significant computational costs and storage are required if the microscale model performs a real-time simulation on every location at each time step of the macroscale simulation, which dramatically reduces the advantage of the multiscale model. To solve this problem, three strategies have been used, as discussed and compared in another paper [57], to refine and reduce the massive information of microscale simulations: the analytical, multi-regression, and RBF network methods. With this multiscale model, the heat transfer coefficient between the capsules and carrying fluid can be calculated instead of being estimated by an empirical equation, and thus the accuracy of the numerical simulation has been found to be significantly increased. As shown by their results, the maximum deviation between the simulation results and the experimental data in [89] was 7.43%.

Although the multiscale mode is more accurate, it is not widely used so far due to its complexity. With the development of the technology, more and more highly accurate calculations will be required, and the multiscale mode will become more and more necessary.

5. Adaptability Analysis and Improvement Direction of Mathematical Model

As discussed above, six types of mathematical models, the single-phase additional source model, single-phase and two-phase equivalent specific heat capacity models, single-phase and two-phase enthalpy models, and the multiscale model, have been established for the heat and mass transfer of the MPCMS. In this section, the research that explicitly provided the deviation in the numerical calculation will be summarized and discussed, to provide reference for the selection of the model. Table 1 summarizes different models for the flow and heat transfer of MEPCS with different application scenarios.

It is found from Table 1, that all these models obtained acceptable accuracy in each research study, and that the two-phase modes are, in general, more accurate than the single-phase model, since they are able to consider the effect of the distribution of the particles on the phase change. However, the deviations of some mathematical models can be improved by some empirical modifications, which may not be reasonable, to ensure that the simulation results were consistent with the experimental data. For example, the accuracy of the additional heat source method is highly dependent on the heat source, which can be empirically modified in the calculation, and the same is for the effective specific heat capacity correlations. Therefore, the conclusions on the accuracy from Table 1 may not be true for the calculations for different physical problems. The choice of mathematical model should be based on the features of the physical problems.

Table 1. Different models for the flow and heat transfer of MEPCS and their performance.

Authors	Physical Problem	Composition of Slurry	Mass Percentage of MPCM	MEPCM Size	Flow Regime	Flow Velocity Range	Reynolds Number Range	Mathematical Model	Model Performance
Charunyakorn et al. [24]	flow and heat transfer of slurry in circular tube	polystyrene/ sodium chloride solution	5–25%	50 μm, 100 μm	laminar flow	-	-	single-phase additional heat source	The deviation between the numerical results and experimental data was between 6% and 12%
Qiu et al. [25]	flow and heat transfer of slurry in circular tube	n-propanol/ pure water	5%, 10%, 20%, 30%	5 μm, 20 μm	laminar flow	10–50 kg/h	335–1295	single-phase additional heat source	The deviation between the numerical results and experimental data was less than 5%
Shaukat et al. [66]	flow and heat transfer of slurry in rectangular microchannel	octadecane/pure water	5–20%	-	laminar flow	1.0–5.0 m/s	168–988	single-phase equivalent specific heat	The maximum deviation between the numerical results and experimental data was 14.6%
Languri et al. [28]	flow and heat transfer of slurry in spiral tube	microcapsule particles/pure water	0%, 5.9%, 10.9%	-	turbulent flow	2.5 m/s	7311–24,160	single-phase equivalent specific heat	The maximum deviation between the numerical results and experimental data was 5%
Hu et al. [27]	flow and heat transfer of slurry in circular tube	microcapsule particles/pure water	10%, 15%, 20%, 25%	50 μm, 100 μm, 250 μm	laminar flow	-	200–1000	single-phase equivalent specific heat	The maximum deviation between the numerical results and experimental data was 6%
Zeng et al. [31]	flow and heat transfer of slurry in circular tube	bromohexade-cane/ amino plastics/pure water	10%, 15%, 20%	8 μm, 40 μm, 80 μm	laminar flow	-	320–1280	single-phase enthalpy method	The maximum deviation between the numerical results and experimental data was 9.4%
Inaba et al. [78]	flow and heat transfer of slurry in rectangular tube	paraffin/pure water	10%, 20%, 30%, 40%	-	laminar flow	-	-	single-phase enthalpy method	The deviation between the numerical results and experimental data was 10%
Hasan [79]	flow and heat transfer of slurry in square microchannel	octadecane/polymethyl methacrylate/pure water	0–20%	-	laminar flow	0.2–3.0 m/s	-	single-phase enthalpy method	The average deviation between the numerical results and experimental data was 2.1%
Feng et al. [29]	flow and heat transfer of slurry in circular tube	n-eicosane/pure water	0%, 5%, 10%, 15%	50 μm, 125 μm,	laminar flow	-	200, 1000	two-phase equivalent specific heat	The numerical results of the two-phase model were more accurate than those of the single-phase model

Table 1. *Cont.*

Authors	Physical Problem	Composition of Slurry	Mass Percentage of MPCM	MEPCM Size	Flow Regime	Flow Velocity Range	Reynolds Number Range	Mathematical Model	Model Performance
Xin et al. [70]	flow and heat transfer of slurry in circular tube	paraffin/pure water	0–25%	-	turbulent flow	-	5000, 8000, 10,000	two-phase equivalent specific heat	The maximum deviation between the numerical results and experimental data was less than 14%
Wu et al. [71]	flow and heat transfer of slurry in circular tube	paraffin/polymethyl methacrylate/pure water	2%, 5%, 8%	10 μm, 50 μm, 100 μm	laminar flow	0.0904 m/s	900	two-phase equivalent specific heat	the numerical results of two-phase mixed model were more accurate than those of single-phase model
Liu et al. [35]	flow and heat transfer of slurry in rectangular tube	octadecane/melamine-formaldehyde resin/pure water	5–20%	50 μm	laminar flow	-	100, 200, 1000	two-phase equivalent specific heat	The maximum deviation between the numerical results and experimental data was 10%
Dai et al. [30]	flow and heat transfer of slurry in square microchannel	octadecane/ polymethyl methacrylate/pure water	5%, 10%, 15%, 20%	-	laminar flow	3.0–5.0 m/s	-	two-phase equivalent specific heat	The deviation between the numerical results and experimental data was less than 1%
Xing et al. [33]	flow and heat transfer of slurry in rectangular microchannel	octadecane/ melamine–formaldehyde resin/pure water	0–25%	-	laminar flow	-	90,167, 300,600	two-phase enthalpy method	The deviation between the numerical results and experimental data was 3.8%
Lin et al. [34]	flow and heat transfer of slurry in circular tube	microcapsule particles/pure water	5–25%	5–1000 μm	laminar flow	1.25 m/s	-	multiscale	The maximum error between numerical results and experimental data was 7.43%.

If the particles are small and uniformly mixed with the carrier fluids, the single-phase model may obtain acceptable accuracy; however, when the capsule particle size is large or the density difference between the capsule and the carrier fluid is large, MEPCS is not a homogeneous fluid, and the homogeneous assumption will cause significant error. Moreover, the distribution of the particles will be affected by the shape of the flow tunnel, and a two-phase model should be used in this case. However, the solid and liquid phases are mathematically regarded as interpenetrated continuums, which may bring unacceptable errors in some cases. When it comes to the choice among the additional heat sources, the specific heat, and enthalpy method, one should clearly understand the shortcomings of different models. For the additional heat source model, a heat source should be introduced, which is sometimes very difficult to obtain, and therefore, they are sometimes not reliable in addition to the complexity they bring to the calculation. For the effective specific heat capacity model, additional experimental tests should be carried out to obtain the expressions of the effective specific heat capacity that highly affect the accuracy of the calculation. For the enthalpy methods, the linear correlations are assumed, which may introduce some error, but they are much more flexible than the other models.

However, all the models, except the multiscale model, are based on the assumption of "homogenization temperature" inside the capsule, which oversimplifies the specific phase change process inside the capsule and sometimes results in significant errors. In addition, it is difficult to describe the subcooling of the phase change material in the capsule with these quasi-continuum models. If the nonlinear behavior is required and the subcooling effect exist, the multiscale model should be preferred. For the highly accurate computation, the multiscale model will become more and more welcomed.

6. Conclusions

The MEPCS is widely used in a variety of energy storage and thermal regulation systems. The design and optimization of these systems using the MEPCS require a full understanding of the heat and mass transfer behavior within the MEPCS. However, the thermal-hydraulic characteristics of the MEPCS are complicated due to the heterogeneous flow and phase transition. The numerical methods are widely used to solve such complicated problems, which however, require accurate mathematical models. This review summarized the mathematical models for the MEPCS, and discussed the advantages and shortcomings of these models, to provide a reference for researchers when they are establishing the mathematical models for the MEPCS. It is concluded that the two-phase models are, in general, more accurate than the single-phase models, however they fail to describe the nonlinear behavior and subcooling effect of the phase change, which can be described in detail by the multiscale models. It is also concluded that the enthalpy models are more flexible than the additional heat source and effective specific heat capacity models, since they do not require any input correlations that are difficult to achieve. In addition, all the macroscopic models discussed in this research are based on the assumption of "homogenization temperature" inside the capsule, which is not able to capture the nonlinear behavior of the phase change. It can be anticipated that the multiscale models will be used more and more widely due to the increasing demand for highly accurate computation in future research.

Author Contributions: Writing—original draft preparation, H.L. (Huyu Li); writing—review and editing, H.L. (Huyu Li), G.Y., H.X., X.H. and H.L. (Huihao Liu); visualization, X.H. and H.L. (Huyu Li); funding acquisition, G.Y. and H.X. All authors have read and agreed to the published version of the manuscript.

Funding: This research was funded by the National Natural Science Foundation of China (grant numbers 51606117 and 41802195), Natural Science Foundation of Shanghai (grant number 20ZR1423300), and the Shanghai Frontiers Science Center of "Full Penetration" Far-Reaching Offshore Ocean Energy and Power.

Data Availability Statement: Not applicable.

Conflicts of Interest: The authors declare no conflict of interest.

References

1. Oró, E.; Gracia, A.D.; Castell, A.; Farid, M.M.; Cabeza, L.F. Review on phase change materials (PCMs) for cold thermal energy storage applications. *Appl. Energy* **2012**, *99*, 513–553.
2. Gao, D.; Wang, S.; Cai, X.; Wang, J.; Li, Y. Preparation of microencapsulated phase change material and its application in microchannels: A review. *Chem. Ind. Eng. Prog.* **2021**, *40*, 5180–5194.
3. Gharsallaoui, A.; Roudaut, G.; Chambin, O.; Voilley, A.; Saurel, R. Applications of spray-drying in microencapsulation of food ingredients: An overview. *Food Res. Int.* **2007**, *40*, 1107–1121.
4. Gibbs, B.F.; Bernard, F.; Kermasha, S. Encapsulation in the food industry: A review. *Int. J. Food Sci. Nutr.* **1999**, *50*, 213.
5. Thaicham, P. Heat transport in a three-stage thermal energy system using phase change material slurries. *Scienceasia* **2010**, *34*, 223–228. [CrossRef]
6. Yang, L.; Liu, S.; Zheng, H. A comprehensive review of hydrodynamic mechanisms and heat transfer characteristics for microencapsulated phase change slurry (MPCS) in circular tube. *Renew. Sustain. Energy Rev.* **2019**, *114*, 109312.
7. Jurkowska, M.; Szczygieł, I. Review on properties of microencapsulated phase change materials slurries (mPCMS). *Appl. Therm. Eng.* **2016**, *98*, 365–373.
8. Huang, M.J.; Eames, P.C.; Mccormack, S.; Griffiths, P.; Hewitt, N.J. Microencapsulated phase change slurries for thermal energy storage in a residential solar energy system. *Renew. Energy* **2011**, *36*, 2932–2939. [CrossRef]
9. Gschwander, S.; Schossig, P.; Henning, H.M. Micro-encapsulated paraffin in phase-change slurries. *Sol. Energy Mater. Sol. Cells* **2005**, *89*, 307–315. [CrossRef]
10. Chen, B.; Wang, X.; Zeng, R.; Zhang, Y.; Wang, X.; Niu, J.; Li, Y.; Di, H. An experimental study of convective heat transfer with microencapsulated phase change material suspension: Laminar flow in a circular tube under constant heat flux. *Exp. Therm. Fluid Sci.* **2008**, *32*, 1638–1646. [CrossRef]
11. Delgado, M.; Lazaro, A.; Mazo, J.; Zalba, B. Review on phase change material emulsions and microencapsulated phase change material slurries: Materials, heat transfer studies and applications. *Renew. Sustain. Energy Rev.* **2012**, *16*, 253–273. [CrossRef]
12. Allouche, Y.; Varga, S.; Bouden, C.; Oliveira, A.C. Experimental determination of the heat transfer and cold storage characteristics of a microencapsulated phase change material in a horizontal tank. *Energy Convers. Manag.* **2015**, *94*, 275–285. [CrossRef]
13. Sabbah, R.; Seyed-Yagoobi, J.; Al-Hallaj, S. Heat transfer characteristics of liquid flow with micro-encapsulated phase change material: Experimental study. *J. Heat Transf.* **2012**, *134*, 044501. [CrossRef]
14. Nazir, H.; Batool, M.; Osorio, F.; Isaza-Ruiz, M.; Xu, X.; Vignarooban, K.; Phelan, P.; Inamuddin; Kannan, A.M. Recent developments in phase change materials for energy storage applications: A review. *Int. J. Heat Mass Transf.* **2019**, *129*, 491–523. [CrossRef]
15. Liu, S.; Li, Y.; Zhang, Y. Mathematical solutions and numerical models employed for the investigations of PCMs' phase transformations. *Renew. Sustain. Energy Rev.* **2014**, *33*, 659–674. [CrossRef]
16. Youssef, Z.; Delahaye, A.; Li, H.; Trinquet, F.; Fournaison, L.; Pollerberg, C.; Doetsch, C. State of the art on phase change material slurries. *Energy Convers. Manag.* **2013**, *65*, 120–132. [CrossRef]
17. Lin, Q. Two-Scale Study on Heat Transfer and Flow Characteristics of Microencapsulated Phase Change Material Suspensions in Pipes. Ph.D. Thesis, Dalian University of Technology, Dalian, China, 2019.
18. Zhang, P.; Ma, Z.W.; Wang, R.Z. An overview of phase change material slurries: MPCS and CHS. *Renew. Sustain. Energy Rev.* **2010**, *14*, 598–614. [CrossRef]
19. Huang, X.; Zhu, C.; Lin, Y.; Fang, G. Thermal properties and applications of microencapsulated PCM for thermal energy storage: A review. *Appl. Therm. Eng.* **2019**, *147*, 841–855. [CrossRef]
20. Liu, X.; Zou, D.; He, R.; Shen, J.; Guo, J.; Hu, Z.; Hu, Y.; Liu, M. Research progress of application of microencapsulated phase change slurry (MEPCS) in heat transport. *Chem. Ind. Eng. Prog.* **2018**, *37*, 1860–1867.
21. Zhi, C.; Fang, G. Preparation and heat transfer characteristics of microencapsulated phase change material slurry: A review. *Renew. Sustain. Energy Rev.* **2011**, *15*, 4624–4632.
22. Li, X.; Li, K.; Qu, D. Progress in research on heat transfer properties of microencapsulated phase change material suspensions. *Funct. Mater.* **2016**, *47*, 4033–4039.
23. Lv, Y.; Dai, S.; Chi, B.; Lu, J.; Han, Y.; Liu, L. Advances in flow and heat transfer of microencapsulated phase change material slurry in mini-pipe. *New Chem. Mater.* **2017**, *45*, 40–42.
24. Charunyakorn, P.; Sengupta, S.; Roy, S. Forced convection heat transfer in microencapsulated phase change material slurries: Flow in circular ducts. *Int. J. Heat Mass Transf.* **1991**, *34*, 819–833. [CrossRef]
25. Qiu, Z.; Li, L. Experimental and Numerical Investigation of Laminar Heat Transfer of Microencapsulated Phase Change Material Slurry (MPCMS) in a Circular Tube with Constant Heat Flux. *Sustain. Cities Soc.* **2020**, *52*, 101786. [CrossRef]
26. Hao, Y.L.; Tao, Y.X. A Numerical Model for Phase-Change Suspension Flow in Microchannels. *Numer. Heat Transf.* **2004**, *46*, 55–77. [CrossRef]
27. Hu, X.; Zhang, Y. Novel insight and numerical analysis of convective heat transfer enhancement with microencapsulated phase change material slurries: Laminar flow in a circular tube with constant heat flux. *Int. J. Heat Mass Transf.* **2002**, *45*, 3163–3172. [CrossRef]

28. Languri, E.M.; Rokni, H.B.; Alvarado, J.; Takabi, B.; Kong, M. Heat transfer analysis of microencapsulated phase change material slurry flow in heated helical coils: A numerical and analytical study. *Int. J. Heat Mass Transf.* **2018**, *118*, 872–878. [CrossRef]
29. Bai, F.; Lu, W.Q. Numerical analysis of laminar forced convection heat transfer in microencapsulated phase change material suspensions. *J. Enhanc. Heat Transf.* **2003**, *10*, 311–322. [CrossRef]
30. Dai, H.; Chen, W. Numerical investigation of heat transfer in the double-layered minichannel with microencapsulated phase change suspension. *Int. Commun. Heat Mass Transf.* **2020**, *119*, 104918. [CrossRef]
31. Zeng, R.; Wang, X.; Chen, B.; Zhang, Y.; Niu, J.; Wang, X.; Di, H. Heat transfer characteristics of microencapsulated phase change material slurry in laminar flow under constant heat flux. *Appl. Energy* **2009**, *86*, 2661–2670. [CrossRef]
32. Sabbah, R.; Farid, M.M.; Al-Hallaj, S. Micro-channel heat sink with slurry of water with micro-encapsulated phase change material: 3D-numerical study. *Appl. Therm. Eng.* **2009**, *29*, 445–454. [CrossRef]
33. Xing, K.Q.; Tao, Y.X.; Hao, Y. Performance evaluation of liquid flow with PCM particles in microchannels. *J. Heat Transf.* **2005**, *127*, 931–940. [CrossRef]
34. Lin, Q.; Wang, S.; Zhang, L. Multi-scale modeling and investigation of thermo-fluidic performance of microencapsulated phase-change material slurry. *J. Energy Storage* **2021**, *37*, 102502. [CrossRef]
35. Liu, L.; Alva, G.; Jia, Y.; Huang, X.; Fang, G. Dynamic thermal characteristics analysis of microencapsulated phase change suspensions flowing through rectangular mini-channels for thermal energy storage. *Energy Build.* **2017**, *134*, 37–51. [CrossRef]
36. Zhang, G.H.; Zhao, C.Y. Thermal and rheological properties of microencapsulated phase change materials. *Renew. Energy* **2011**, *36*, 2959–2966. [CrossRef]
37. Sabbah, R.; Seyed-Yagoobi, J.; Al-Hallaj, S. Heat Transfer characteristics of liquid Flow with micro-encapsulated phase change material: Numerical study. *J. Heat Transf.* **2011**, *133*, 121702. [CrossRef]
38. Li, L.; Zou, D.; Zhan, J. New Progress in convection heat transfer characteristics of microencapsulated phase change material suspension. *Mater. Rev.* **2015**, *29*, 55–59.
39. Roy, S.K.; Avanic, B.L. Turbulent heat transfer with phase change material suspensions. *Int. J. Heat Mass Transf.* **2001**, *44*, 2277–2285. [CrossRef]
40. Goel, M.; Roy, S.K.; Sengupta, S. Laminar forced convection heat transfer in microcapsulated phase change material suspensions. *Int. J. Heat Mass Transf.* **1994**, *37*, 593–604. [CrossRef]
41. Liu, L.; Zhu, C.; Fang, G. Numerical evaluation on the flow and heat transfer characteristics of microencapsulated phase change slurry flowing in a circular tube. *Appl. Therm. Eng.* **2018**, *144*, 845–853. [CrossRef]
42. Guyer, E.C. Handbook of Applied Thermal Design. In *Handbook of Applied Thermal Design*; CRC Press: Boca Raton, FL, USA, 1999.
43. Maxwell, J. A Treatise On Electricity and Magnetism. *Nature* **2014**, *7*, 478–480.
44. Yuan, K.; Wang, H.; Liu, J.; Fang, X.; Zhang, Z. Novel slurry containing graphene oxide-grafted microencapsulated phase change material with enhanced thermo-physical properties and photo-thermal performance. *Sol. Energy Mater. Sol. Cells* **2015**, *143*, 29–37. [CrossRef]
45. Liu, C.; Ma, Z.; Wang, J.; Li, Y.; Rao, Z. Experimental research on flow and heat transfer characteristics of latent functional thermal fluid with microencapsulated phase change materials. *Int. J. Heat Mass Transf.* **2017**, *115*, 737–742. [CrossRef]
46. Kong, M.; Alvarado, J.L.; Terrell, W.; Thies, C. Performance characteristics of microencapsulated phase change material slurry in a helically coiled tube. *Int. J. Heat Mass Transf.* **2016**, *101*, 901–914. [CrossRef]
47. Chen, L.; Wang, T.; Zhao, Y.; Zhang, X.-R. Characterization of thermal and hydrodynamic properties for microencapsulated phase change slurry (MPCS). *Energy Convers. Manag.* **2014**, *79*, 317–333. [CrossRef]
48. Wang, L.; Zhang, J.; Wang, Y.; Lin, X.; Xie, N.; Chen, H. Experimental study on natural convective heat transfer of tube immersed in microencapsulated phase change material suspensions. *Appl. Therm. Eng. Des. Process. Equip. Econ.* **2016**, *99*, 583–590. [CrossRef]
49. Delgado, M.; Lázaro, A.; Pealosa, C.; Zalba, B. Experimental analysis of the influence of microcapsule mass fraction on the thermal and rheological behavior of a PCM slurry. *Appl. Therm. Eng.* **2014**, *63*, 11–22. [CrossRef]
50. Carreau, P.J. Rheological equations from molecular network theories. *Trans. Soc. Rheol.* **2000**, *16*, 99–127. [CrossRef]
51. Vand, V. Theory of viscosity of concentrated suspensions. *Nature* **1945**, *155*, 364–365. [CrossRef]
52. Mulligan, J.C.; Colvin, D.P.; Bryant, Y.G. Microencapsulated phase-change material suspensions for heat transfer in spacecraft thermal systems. *J. Spacecr. Rocket.* **2012**, *33*, 278–284. [CrossRef]
53. Wang, X.; Niu, J.; Yi, L.; Xin, W.; Chen, B.; Zeng, R.; Song, Q.; Zhang, Y. Flow and heat transfer behaviors of phase change material slurries in a horizontal circular tube. *Int. J. Heat Mass Transf.* **2007**, *50*, 2480–2491. [CrossRef]
54. Ho, C.J.; Lin, J.F.; Chiu, S.Y. Heat transfer of solid-liquid phase-change material suspensions in circular pipes: Effects of wall conduction. *Numer. Heat Transf. Appl.* **2004**, *45*, 171–190.
55. Hao, Y.; Lu, J. Parametric Study for the Phase-Change Process of Liquid Flow with Microencapsulated PCM Particles in Microchannels. *Proc. Int. Conf. Integr. Commer. Micro Nanosyst.* **2007**, *42657*, 853–860.
56. Tao, W.Q.; He, Y.L. Multiscale simulations of heat transfer and fluid flow problems. *J. Heat Transf. Trans.* **2012**, *9*, 150–157.
57. Lin, Q.; Wang, S.; Wang, J. Multi-scale modeling of heat transfer during phase change of microencapsulated slurry and the coupling strategy between different scales. *J. Chem. Eng. Chin. Univ.* **2019**, *33*, 81–90.
58. Yun, H. Study on Flow and Heat Transfer Characteristics of Single Phase in Mini-Channels. Ph.D. Thesis, Shandong University, Jinan, China, 2007.

59. Ye, S.; Wang, C.; Wu, Y.; Guo, Y.; Zhang, X.-J. Microencapsulation Technology and It's Application in Phase Change Materials. *Guangzhou Chem.* **2004**, *29*, 34–38+45.
60. Zhang, S.; Niu, J. Two performance indices of TES apparatus: Comparison of MPCM slurry vs. stratified water storage tank. *Energy Build.* **2016**, *127*, 512–520. [CrossRef]
61. Ahuja, A.S. Augmentation of heat transport in laminar flow of polystyrene suspensions. I. Experiments and results. *J. Appl. Phys.* **1975**, *46*, 3408–3416. [CrossRef]
62. Pan, A.; Wang, J.; Zhang, X. Numerical Analysis of Phase-Change Heat Transfer Characteristics Using Effective Heat Capacity Method and Enthalpy Method. *Comput. Simul.* **2014**, *31*, 315–319.
63. Seyf, H.R.; Zhou, Z.; Ma, H.B.; Zhang, Y. Three dimensional numerical study of heat-transfer enhancement by nano-encapsulated phase change material slurry in microtube heat sinks with tangential impingement. *Int. J. Heat Mass Transf.* **2013**, *56*, 561–573. [CrossRef]
64. Kong, M. Flow and Heat Transfer Characteristics of Microencapsulated Material Slurry in a Coil Heat Exchanger. *J. Heat Transf.* **2015**, *137*, 071801. [CrossRef]
65. Ran, F.; Xu, C.; Chen, Y.; Cong, R.; Fang, G. Numerical flow characteristics of microencapsulated phase change slurry flowing in a helically coiled tube for thermal energy storage. *Energy* **2021**, *223*, 120–128. [CrossRef]
66. Shaukat, R.; Kamran, M.S.; Imran, S.; Anwar, Z.; Ali, H. Numerical investigation of melting heat transfer during microencapsulated phase change slurry flow in microchannels. *J. Enhanc. Heat Transf.* **2019**, *26*, 551–575. [CrossRef]
67. Mahian, O.; Kolsi, L.; Amani, M.; Estellé, P.; Ahmadi, G.; Kleinstreuer, C.; Marshall, J.S.; Siavashi, M.; Taylor, R.A.; Niazmand, H. Recent advances in modeling and simulation of nanofluid flows-Part I: Fundamentals and theory. *Phys. Rep.* **2018**, *790*, 1–48. [CrossRef]
68. Mohian, O.; Kolsi, L.; Amani, M.; Estelle, P.; Ahmadi, G.; Kleinstreuer, C.; Marshall, J.S.; Taylor, R.A.; Abu-Nada, E.; Rashidi, S.; et al. Recent advances in modeling and simulation of nanofluid flows—Part II: Applications-ScienceDirect. *Phys. Rep.* **2019**, *791*, 1–59. [CrossRef]
69. Ma, F.; Zhang, P.; Shi, X.J.; Yan, J. Investigation of thermo-fluidic performance of phase change material slurry and energy transport characteristics. *Appl. Energy* **2018**, *227*, 643–654. [CrossRef]
70. Xin, W.; Zhang, Y.; Hu, X. Turbulent Heat Transfer Enhancement of Microencapsulated Phase Change Material Slurries with Constant Wall Heat Flux. *J. Enhanc. Heat Transf.* **2003**, *11*, 15–32. [CrossRef]
71. Wu, X.; Yang, Z.; Chen, Y.; Duan, Y. Simulation studies on heat transfer characteristics of PCM microencapsulated fluids based on discrete phase model. *J. Chem. Ind. Eng.* **2020**, *71*, 1491–1501.
72. Ho, C.J.; Huang, J.B.; Tsai, P.S.; Yang, Y.M. Water-based suspensions of Al_2O_3 nanoparticles and MEPCM particles on convection effectiveness in a circular tube. *Int. J. Therm. Sci.* **2011**, *50*, 736–748. [CrossRef]
73. Liang, W.; Lin, G. Experimental study on the convective heat transfer behavior of microencapsulated phase change material suspensions in rectangular tube of small aspect ratio. *Heat Mass Transf.* **2012**, *48*, 83–91.
74. Wei, X.; Joshi, Y.; Patterson, M.K. Experimental and Numerical Study of a Stacked Microchannel Heat Sink for Liquid Cooling of Microelectronic Devices. *J. Heat Transf.* **2007**, *129*, 1432–1444. [CrossRef]
75. Dammel, F.; Stephan, P. Heat Transfer to Suspensions of Microencapsulated Phase Change Material Flowing Through Minichannels. *J. Heat Transf.* **2012**, *134*, 020907. [CrossRef]
76. Dai, H.; Chen, W.; Cheng, Q.; Liu, Y.; Dong, X. Analysis of thermo-hydraulic characteristics in the porous-wall microchannel with microencapsulated phase change slurry. *Int. J. Heat Mass Transf.* **2021**, *165*, 120634. [CrossRef]
77. Dai, H.; Chen, W.; Dong, X.; Liu, Y.; Cheng, Q. Thermohydraulic performance analysis of graded porous media microchannel with microencapsulated phase change material suspension. *Int. J. Heat Mass Transf.* **2021**, *176*, 121459. [CrossRef]
78. Inaba, H.; Zhang, Y.; Horibe, A. Transient Heat Storage Characteristics on Horizontal Rectangular Enclosures Filled with Fluidity Slurry of Micro-encapsulated Phase-change-material Dispersed in Water. *J. Therm. Sci. Technol.* **2006**, *1*, 66–77. [CrossRef]
79. Hasan, M.I. Numerical investigation of counter flow microchannel heat exchanger with MEPCM suspension. *Appl. Therm. Eng.* **2011**, *31*, 1068–1075. [CrossRef]
80. Farid, M.; Smith, M.; Sabbah, R.; Hallaj, S.A. Miniaturized Refrigeration System with Advanced PCM Micro Encapsulation Technology. In Proceedings of the ASME International Conference on Nanochannels, Puebla, Mexico, 18–20 June 2007.
81. Abhijith, M.S.; Venkatasubbaiah, K. Numerical investigation on laminar forced convection of MEPCM-water slurry flow through a micro-channel using Eulerian-Eulerian two-phase model. *Therm. Sci. Eng. Prog.* **2021**, *22*, 100803.
82. Lian, C.; Wang, Y.; Li, Q.; Li, H.; He, X. Numerical investigation on the performance of microencapsulated phase change material suspension applied to liquid cold plates. *Numer. Heat Transf. Part A Appl.* **2019**, *75*, 342–358. [CrossRef]
83. Inaba, H.; Kim, M.J.; Horibe, A. Melting Heat Transfer Characteristics of Microencapsulated Phase Change Material Slurries with Plural Microcapsules Having Different Diameters. *J. Heat Transf.* **2004**, *126*, 558–565. [CrossRef]
84. Afsahi, M.M.; Mohebbi, A.; Sattari, H.; Yancheshme, A.A. CFD simulation of melting process of phase change materials (PCMs) in a spherical capsule. *Int. J. Refrig.* **2017**, *73*, 209–218.
85. Liu, M.J.; Fan, L.W.; Zhu, Z.Q.; Feng, B.; Zhang, H.C.; Zeng, Y. A volume-shrinkage-based method for quantifying the inward solidification heat transfer of a phase change material filled in spherical capsules. *Appl. Therm. Eng.* **2016**, *108*, 1200–1205. [CrossRef]

86. Lin, Q.; Wang, S.; Ma, Z.; Wang, J.; Zhang, T. Lattice Boltzmann simulation of flow and heat transfer evolution inside encapsulated phase change materials due to natural convection melting. *Chem. Eng. Sci.* **2018**, *189*, 154–164. [CrossRef]
87. Abdulle, A.; Weinan, E.; Engquist, B.; Vanden-Eijnden, E. The heterogeneous multiscale method. *Acta Numer.* **2012**, *21*, 1–87. [CrossRef]
88. Li, J.; Kwauk, M. Exploring complex systems in chemical engineering—The multi-scale methodology. *Chem. Eng. Sci.* **2003**, *58*, 521–535. [CrossRef]
89. Yamagishi, Y.; Takeuchi, H.; Pyatenko, A.T.; Kayukawa, N. Characteristics of microencapsulated PCM slurry as a heat-transfer fluid. *AIChE J.* **2010**, *45*, 696–707. [CrossRef]